PAPER 25 (SESSION II)

The fracture behavior of crystalline solids—an atomistic approach

ROGER CHANG
Science Center, North American Rockwell Corp.,
Thousand Oaks, California, U.S.A.

Summary
A mathematical relaxation method developed by the author to study the core structures of screw and edge dislocations in crystalline solids was used to investigate the configurations and energies of atoms and stress induced crack opening displacements in solids of different crystal structures. Single crystals of the material containing initially an atomically sharp and through crack were subjected to external tensile stresses applied normal to the crack under plain strain conditions. The results obtained for body-centered cubic and face-centered cubic iron, for which an empirical two-body interatomic potential is available, are presented. Under no externally applied stress, the BCC specimens retained the vacancy sheet configuration with very little relaxation while the FCC specimens relaxed considerably more around the vacancy sheet. Under applied tensile stress, the BCC specimens exhibited discontinuous crack motion when the effective stress at the crack tip reached a critical value while the FCC specimens showed smooth crack opening displacement with increasing applied stress. It is believed that the above differences are not very sensitive to details of the interatomic potential and are a genuine reflection of the differences in crystal structure.

The apparent success of the theoretical physicists in applying pseudopotentials to study the material properties of simple metals and semiconductors suggests that the same approach can be used to investigate the mechanical properties of solids, particularly the fracture behavior of metals. The crux of the problem is the availability of rigorous and realistic interatomic potentials. This is indeed fortunate since the pseudopotential method implies that, at constant volume, an effective two-body potential, combining the structure- and volume-dependent parts of the ion-ion, ion-electron and electron-electron potentials, can be used [1]. The volume-dependent but structure-independent parts of the potentials can be excluded since at constant volume they contribute a constant energy term independent of the details of the atom configurations.

For simple metals such as sodium, magnesium, aluminum, etc., effective two-body potentials can indeed be constructed via the pseudo-potential approach. For transition metals, however, such a step is not yet possible. If the potentials could be constructed some other way so as to avoid quantum-mechanical considerations, it might not be too bad, as a first order approximation, to treat all metals alike. With this notion in mind we therefore choose to express the two-body potential empirically

in power series of the interatomic separation and match the potential with the elastic properties of the material. Explicit relationships exist between a two-body interatomic potential and the second and third order elastic constants for body-centered cubic and face-centered cubic metals [2]. The interatomic potential so constructed for body-centered cubic iron is shown in Fig. 1. The details of obtaining this potential from experimental elastic constants data has been discussed by the author elsewhere [3]. Although the potential shown in Fig. 1 was constructed for body-centered cubic iron, there appears to be no serious objection, as a first order approximation, to its being used also for face-centered cubic iron [4]. Relaxational methods employing the interatomic potential to study the configurations and energies of atoms near the core region of edge and screw dislocations in body-centered cubic iron have been reported by the author in two separate publications [5, 6]. The method has since been modified to investigate the fracture and crack displacement behavior of iron in both the BCC and FCC form. We report here our preliminary findings on this subject.

Some typical crystallites containing an atomically sharp and through crack (the equivalence of a planar vacancy sheet) for the BCC structure are shown in Fig. 2. The X-, Y-, and Z- directions are parallel to the three cube edges of the BCC cell. The projections of two neighboring plane of atoms onto the XY plane are shown in Fig. 2. The outer boundary coordinates in both the X- and Y- directions (located between the solid and dotted rectangles shown in Fig. 2) were fixed according to anisotropic elasticity by substituting the central vacancy sheet with a pair of edge dislocations with opposite Burgers vectors in the X- direction. Anisotropic elasticity solutions of the displacements in the X- and Y- directions for a single edge dislocation and an edge dislocation dipole of width $2d$ are presented in Table 1. The coordinates of all atoms both outside and inside the crystallite were computed according to these equations. The relaxed coordinates of all the atoms inside the crystallite were then obtained by means of repeated iterative procedures listed in Table 2 according to the given interatomic potential.

In some instances a tensile strain was imposed in the X- direction: this was accomplished by displacing all the atoms (including the boundary atoms) in the X- direction by an amount proportional to its distance from the mid-plane (the vacancy sheet). The relaxed coordinates of all the atoms inside the crystallite were again obtained after the application of strain according to the same interatomic potential. The average distance between the two atom planes next to the vacancy sheet (crack opening displacement) was monitored as a function of the applied tensile strain. It is noted that the application of an elastic strain induces a slight change in the volume of the crystallite. The computed results are therefore only

approximate at small strains and probably are meaningless at large imposed strains.

In other instances a few evenly spaced carbon atoms (about ten per cent of the total number of vacancies) were added to the vacancy sheet in order to probe the effect of strongly interacting impurities. The empirical potential between the iron and carbon atoms reported by Johnson was used [7].

Fig. 3 shows typically the relaxed atom coordinates (projection of two neighboring atom planes) for the BCC and FCC crystallites near the vacancy sheet under no externally applied tensile strain. It is noted that for the BCC lattice (upper diagram of Fig. 3) the vacancy sheet maintained nearly its original shape while there were considerable atom displacements around the vacancy sheet for the FCC lattice (lower diagram of Fig. 3). In fact the vacancy sheet in the FCC lattice had nearly collapsed except near the crack tip giving rise to a 'stacking fault' two atom-plane thick separated by a distance slightly less than the nearest neighbor spacing.

Fig. 4 shows the crack opening displacement (in direction of applied tensile strain normal to the crack) versus the applied stress (converted from the imposed elastic strain according to linear elasticity) for a BCC crystallite with and without the inclusion of carbon atoms in the vacancy sheet. Fig. 5 shows the same for a FCC crystallite. It is interesting to note that the applied stress-crack opening displacement plots are in many respects similar to the macroscopic stress-strain curves for these materials.

The results presented above suggest that in BCC iron atomically sharp cracks tend to stay sharp (note that the effect of temperature and lattice vibrations has not been considered here) while in FCC iron the opposite seems to be true. Intuitively we feel that there is theoretical justification for brittle fracture and plain strain stress intensity factor K_{Ic} for BCC iron but not for FCC iron. For BCC iron it is possible to compute both the theoretical fracture strength and theoretical shear strength from our data; the same could not be accomplished for FCC iron. There appears to be no theoretical basis to consider K_{Ic} for FCC iron and probably also for other FCC metals. In other words, the stress intensity factors for FCC metals cannot be uniquely defined and are dependent on geometrical and other factors.

One of the important conclusions reached in this investigation is the important roles played by the crystal structure of a solid in affecting its fracture behavior. It appears intuitively to us also that this gross dependence on the crystal structure may not be very sensitive to small changes in the interatomic potential. Further verification of the effect of crystal structure on the fracture behavior of solids must await more elaborated treatment with better and more rigorous interatomic potentials than that used in the present investigation.

References

1. HARRISON, W. A., 'Pseudo-potentials in the theory of metals', W. A. Benjamin Press, 1966.
2. COLDWELL-HORSFALL, R. A., *Phys. Rev.*, vol. 129, p. 22, 1963.
3. CHANG, R. & GRAHAM, L. J., 'Calculation of the properties of vacancies and interstitials', *National Bureau of Standards Misc.*, Publication no. 287, p. 53, 1966.
4. JOHNSON, R. A., 'Calculation of the properties of vacancies and interstitials', *National Bureau of Standards Misc.*, Publication no. 287, p. 39, 1966.
5. CHANG, R. & GRAHAM, L. J., *Phys. Stat. Solidi*, vol. 18, p. 99, 1966.
6. CHANG, R., *Phil. Mag.*, vol. 16, p. 1021, 1967.
7. JOHNSON, R. A., DIENES, G. J. & DAMASK, A. C., *Acta Met.*, vol. 12, p. 1215, 1964.

Table 1
Analytical solutions for the displacements of an edge dislocation and a pair of edge dislocations of opposite sign in cubic solids according to anisotropic elasticity.

Single edge dislocation:

$$U_X = R\,\frac{-b}{4\pi \sin 2\alpha}\left[\frac{C_{11}\,e^{i2\alpha} - C_{12}}{C_{11}}\right]\ln\frac{x + e^{i\alpha}\,y}{x - e^{i\alpha}\,y}$$

$$U_Y = R\,\frac{-b}{4\pi \sin 2\alpha}\left[\frac{C_{11}\,e^{i2\alpha} - C_{12}}{C_{11}}\right]\left[\frac{C_{44}\,e^{i\alpha} + C_{11}\,e^{-i\alpha}}{C_{12} + C_{44}}\right]\ln(x^2 - e^{i2\alpha}\,y^2)$$

$$\cos 2\alpha = \frac{2C_{12}C_{44} + C_{12}^2 - C_{11}^2}{2C_{11}C_{44}}$$

R = Real value of

Pair of edge dislocations of separation 2d:

$$\frac{U_X}{b} = \frac{(C_{12}/C_{11}) - \cos 2\alpha}{8\pi \sin \alpha}\left[\ln\frac{x^2 + (y-d)^2 + 2x(y-d)\cos\alpha}{x^2 + (y-d)^2 - 2x(y-d)\cos\alpha} + \ln\frac{x^2 + (-y-d)^2 + 2x(-y-d)\cos\alpha}{x^2 + (-y-d)^2 - 2x(-y-d)\cos\alpha}\right]$$

$$+\frac{1}{4\pi}\left[\tan^{-1}\frac{(y-d)\sin\alpha}{x + (y-d)\sin\alpha} + \tan^{-1}\frac{(y-d)\sin\alpha}{x - (y-d)\sin\alpha} + \tan^{-1}\frac{(-y-d)\sin\alpha}{x + (-y-d)\sin\alpha} + \tan^{-1}\frac{(-y-d)\sin\alpha}{x - (-y-d)\sin\alpha}\right]$$

$$\frac{U_Y}{b} = \frac{1}{8\pi \sin\alpha}\left[\frac{4C_{44}\sin^2\alpha}{C_{12} + C_{44}} - \frac{(C_{11} - C_{12})}{C_{11}}\left(\frac{C_{11} + C_{44}}{C_{12} + C_{44}}\right)\right]\left[\ln\frac{\sqrt{x^4 - 2x^2(y-d)^2\cos 2\alpha + (y-d)^4}}{\sqrt{x^4 - 2x^2(-y-d)^2\cos 2\alpha + (-y-d)^4}}\right]$$

$$-\frac{1}{8\pi\cos\alpha}\left[\frac{4C_{44}\cos^2\alpha}{C_{12} + C_{44}} + \frac{(C_{11} + C_{12})}{C_{11}}\left(\frac{C_{11} - C_{44}}{C_{12} + C_{44}}\right)\right]\left[\tan^{-1}\frac{(y-d)^2\sin 2\alpha}{x^2 - (y-d)^2\cos 2\alpha} - \tan^{-1}\frac{(-y-d)^2\sin 2\alpha}{x^2 - (-y-d)^2\cos 2\alpha}\right]$$

Table 2
Summary of iterative procedures

1. Obtain coordinates of atom I.J.K. and its N neighbors.

2. Compute forces acting on atom I.J.K. by the N neighbors $\left(F = -\frac{\partial \phi(r)}{\partial r}\right)$.

3. Obtain new coordinates of atom I.J.K. such that the sum total of forces from step 2 is zero ($\sum_{1}^{N} F = 0$).

4. Go to next atom and repeat steps 1 to 3.

5. Repeat step 4 until whole array is covered.

6. Repeat steps 1 to 5 until the changes in coordinates of all atoms in array between successive iterations are within preset limits (0·000001Å).

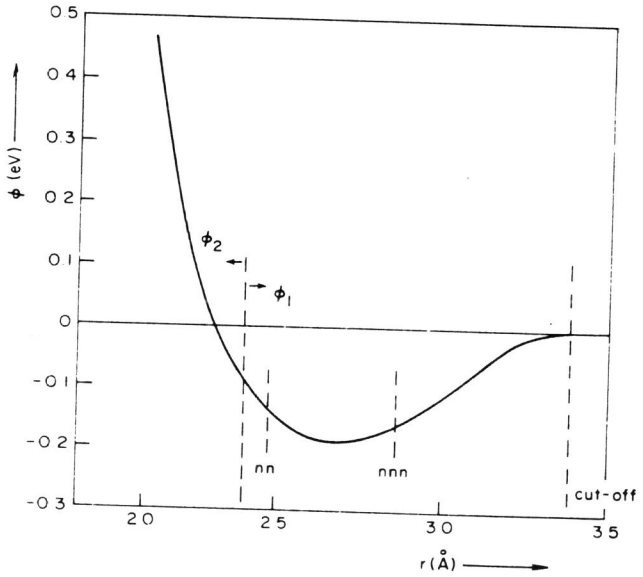

Fig. 1. Iron-iron two-body interatomic potential.

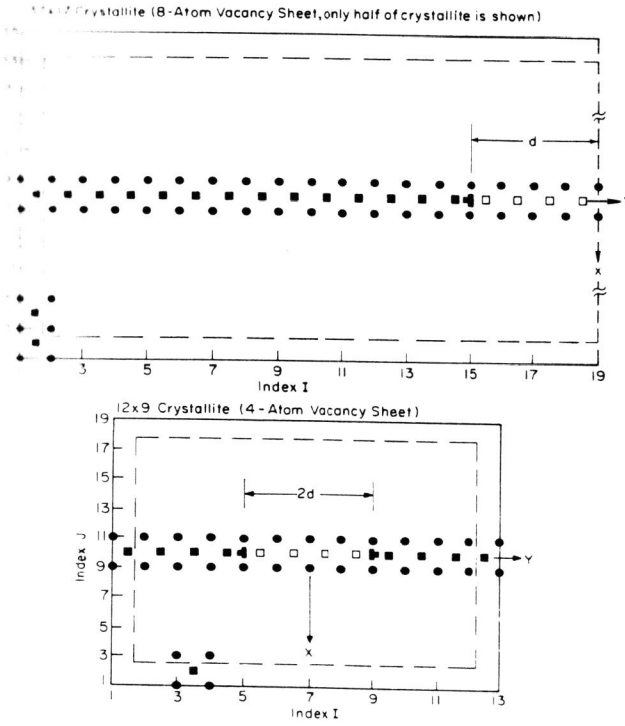

Fig. 2. Typical crystallites used in this study (BCC lattice, circles and squares are respectively projections of two neighboring plane of atoms; open squares are vacant lattice sites; I in units of a_0, J in units of $a_0/2$, a_0 being the lattice parameter).

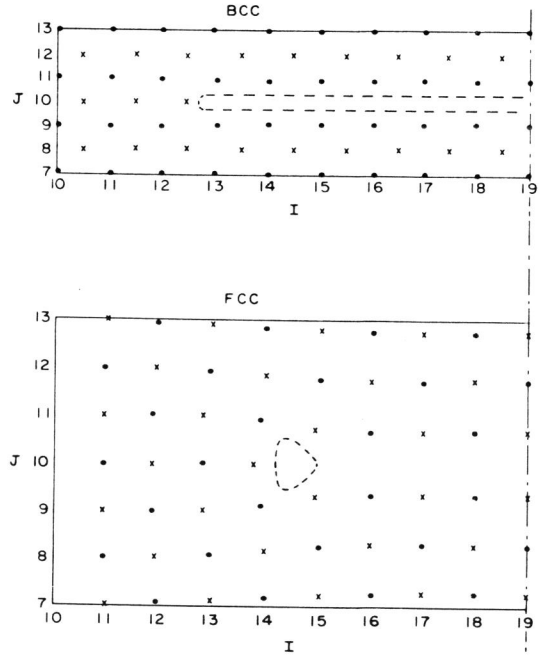

Fig. 3. Relaxed atom coordinates (projections of two neighboring atom planes) near a vacancy sheet for BCC (upper diagram) and FCC (lower diagram) crystallites under no applied stress (I in units of a_0 and J in units of $a_0/2$ for BCC case; both I and J in units of $a_0/2$ for FCC case; only half of crystallite is shown; crosses and dots are projections of atoms from two neighboring planes).

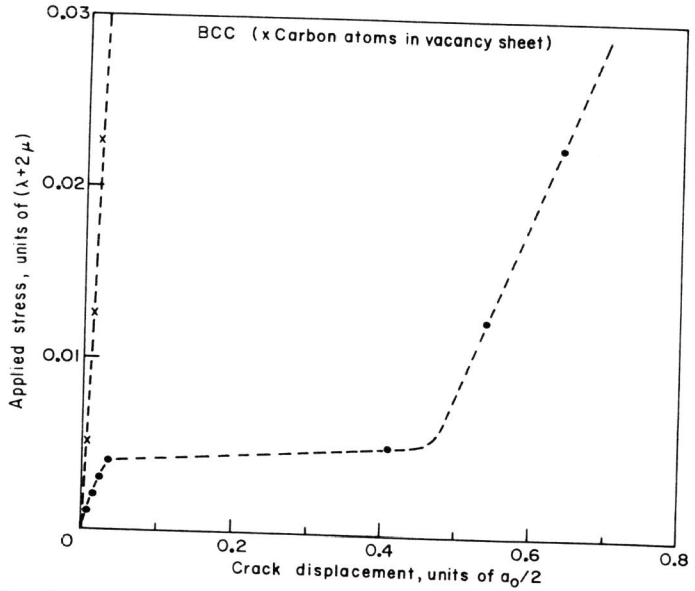

Fig. 4. Crack opening displacement versus applied tensile stress for BCC iron containing a vacancy sheet according to the relaxation method.

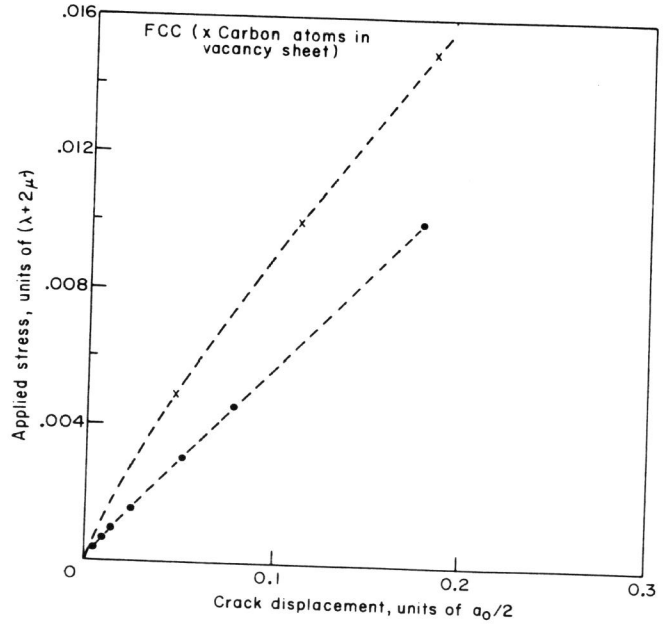

Fig. 5. Same as Fig. 4, FCC iron.